Exploring the Dark Side of the Universe

Sneha Vireshwar Dixit | Advisor : Dr. Digesh Raut

Senior Capstone Experience, Spring 2023

Department of Physics at Washington College

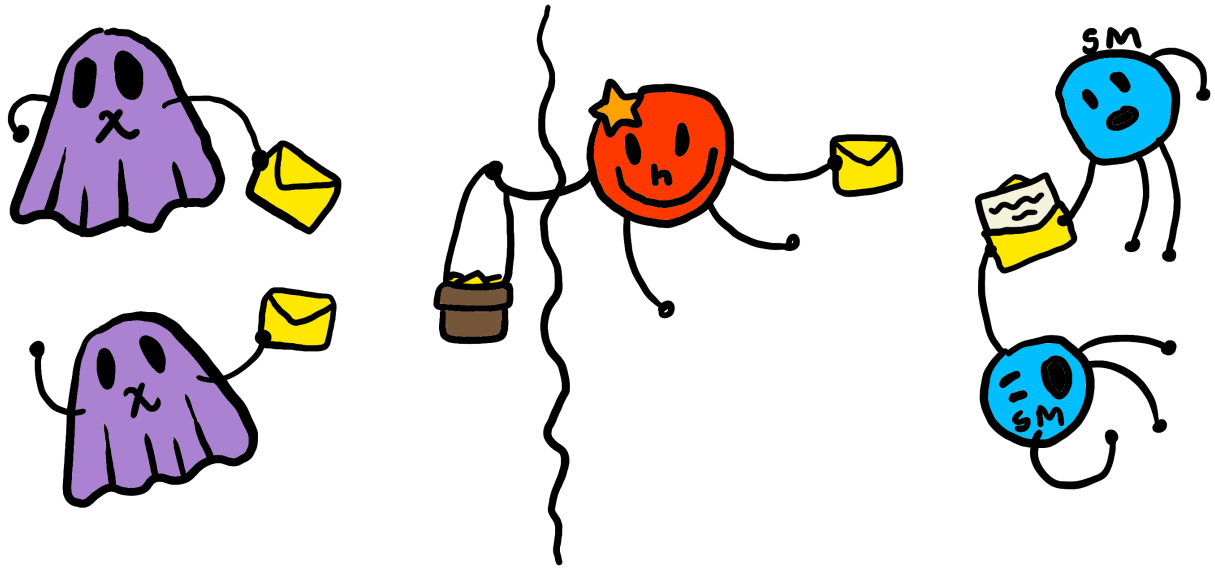

Abstract

Despite accounting for 85% of all matter in the universe, there is no viable dark matter candidate within the standard model of particle physics. Higgs Portal dark matter is one of the most favored candidates for dark matter because all interactions between dark matter and standard model particles in this model are mediated by the standard model Higgs Boson. The interactions are uniquely determined by the dark matter coupling to the standard model Higgs Boson (λ), and dark matter mass (m_χ). By numerically solving the Boltzmann equation, we evaluate λ as a function of m_χ for scenarios where Higgs Portal dark matter accounts for 100%, 70% and 50% of the total dark matter abundance in the universe. We then impose constraints from the LUX-ZEPLIN(LZ) experiment, which provides the most severe bound on the inelastic scattering cross-section between dark matter and heavy nuclei. In the case of Higgs Portal dark matter, this cross-section is determined by the same two parameters - λ and m_χ. After taking into account the direct detection bounds, we show that that only a small region around the resonance, where $m_\chi \approx \frac{m_h}{2}$, is allowed.

1 Introduction

The term 'dark matter' was first coined in the 1930s by Swiss astrophysicist Fritz Zwicky. Zwicky was studying the Coma Cluster when he observed the galaxies at the edge of the cluster had enough velocity to escape the gravitational pull of the cluster. According to the Virial Theorem, the velocity of a galaxy depends on the gravitational force it experiences. For a cluster of given mass, the velocity of a galaxy should fall off as $v \propto \frac{1}{\sqrt{r}}$, where r is the distance from the center of the cluster. Zwicky proposed the existence of invisible matter ('dark' matter) within the cluster to account for the additional gravitational pull needed to explain the higher velocity of galaxies at the edge of the cluster [2].

In the 1960s, Vera Rubin observed similar behavior at the scale of galaxies. Rubin observed that stars at the edge of galaxies move with much greater velocity than predicted by Newtonian gravity[10]. A uniformly distributed dark matter halo surrounding the galaxy can explain the constant velocity of the stars at the edge of the galaxy (see Figure 1).

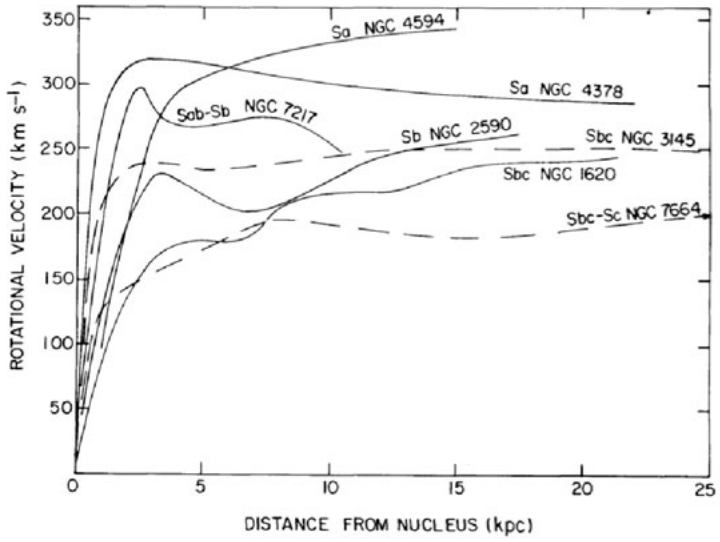

Figure 1: Galaxy rotation curves reproduced from Vera Rubin's work. [10]

Following Rubin's work, various cosmological observations have confirmed the existence of dark matter. For instance, a sufficiently strong gravitational field can cause light to deflect in a phenomenon called gravitational lensing. This has been used to track the distribution of dark matter in the universe (see Figure 2).[2].

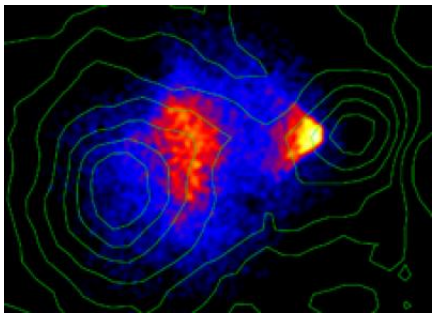

Figure 2: Dark matter mass contours in the Bullet Cluster, observed via gravitational lensing.
Image : Chandra X-Ray Telescope

The anisotropies in the cosmic microwave background (CMB) provide the most precise measurement of the abundance of dark matter in the universe. The CMB is the faint radiation from just after the Big Bang. Dark matter perturbations leave visible ripples, or anisotropies, in the CMB. The current estimate is that dark matter constitutes roughly 85% of all matter in the universe [9].

Evidence from experiments (including some mentioned above) tells us that dark matter is 'cold' or non-relativistic and interacts extremely weakly with standard model particles. The standard model of particle physics is currently the most widely accepted theory that describes the basic building blocks of our universe. Even with all the astrophysical and cosmological evidence, the precise nature of dark matter remains unknown. Since the standard model has no viable dark matter candidiate, the standard model needs to be extended to account for the existence of dark matter. One of the most well-known dark matter candidates is the so-called WIMP (Weakly Interacting Massive Particle) dark matter. Other dark matter candidates besides WIMPs include primordial black holes, axions, neutrinos, strongly interacting massive particles, and even topological defects in the fabric of space-time [1].

In this thesis, we focus on scalar WIMP dark matter, particularly, the so-called 'Higgs-Portal' dark matter in which dark matter interacts with standard model particles solely through the interactions mediated by the standard model Higgs Boson. We begin by introducing the Boltzmann equation, which is used to evaluate the abundance of dark matter. The Boltzmann equation takes the cross-section for dark matter interactions as an input. Using Feynman diagrams, we illustrate the process of evaluating the cross-section for one of these processes. Using the cross-section, we solve the Boltzmann equation to identify the model parameters for various dark matter abundance values. We impose the constraint from direct detection experiments and then identify the allowed parameter space.

2 The Boltzmann Equation

The Boltzmann equation describes the evolution of dark matter abundance with time [8]. We have [7][12]

$$\frac{dY}{dx} = -\frac{\Gamma}{H(x)}(Y(x)^2 - Y_{EQ}^2),$$

$x = \dfrac{m_\chi}{T}$ (m_χ = mass of dark matter, T = temperature of the universe),
$Y = \dfrac{n}{s}$ (n = number density of dark matter, s = entropy density),
$\Gamma = n_{EQ}\langle\sigma v\rangle$,
n_{EQ} = equilibrium number density of dark matter,
σ = cross-section of dark matter interaction with standard model particles,
v = relative velocity between dark matter particles and standard model particles,
$H(x)$ = Hubble parameter.

Here, Γ is the interaction rate between dark matter and standard model particles, $Y(x)$ is the yield of dark matter, and Y_{EQ} is the yield of particles in thermal equilibrium. The cross-section, σ, quantifies the probability of the interaction taking place. $H(x)$ encodes the expansion of the universe. Since x is inversely proportional to temperature, and so a greater value of x denotes greater time in the expanding universe.

Once we know $\langle\sigma v\rangle$, we can solve the Boltzmann equation to evaluate $Y(x)$. The relic abundance ($\Omega_{DM}h^2$) of dark matter is given by

$$\Omega_{DM}h^2 = \frac{Y_\infty m_\chi h^2}{\rho_c}$$

Here, $h = \frac{H_o}{100} \approx 0.7$, where H_o is the Hubble parameter, $\rho_c = \frac{3H^2}{8\pi G}$ is the critical density (where G is the gravitational constant), Y_∞ is the value of Y at present, which is obtained by solving the Boltzmann

equation in the limit $t \longrightarrow \infty$. In order for dark matter to constitute 85% of all matter in the universe, we need $\Omega_{DM}h^2 = 0.11$[7], or equivalently, $Y_\infty = 3.90436 * 10^{-12} m_\chi^{-1}$.

3 Higgs Portal Dark Matter

In particle physics, symmetry properties of particles govern their interactions. We focus on scalar dark matter particles, particularly, so-called Higgs Portal dark matter, where, the symmetry forbids dark matter interactions with particles that are not the standard model Higgs Boson.

A Feynman diagram is a spacetime diagram used to represent interactions between elementary particles. The lines in the diagram correspond to elementary particles, and the vertices represent interactions between them. A dashed line is used for scalars (like our dark matter candidate, or the Higgs Boson), and a solid line is used for fermions. Constants associated denote the strength of the interaction.[3]

In Figure 3, the left panel shows the Feynman rules relevant for the dark matter interaction with standard model particles. Here, χ are scalar dark matter particles, h is the standard model Higgs Boson, and 'SM' are standard model final state particles. λ is the coupling constant that quantifies the probability of interactions between χ and h, v_H is the vacuum expectation value of the standard model Higgs Boson, and Y_{SM} is the coupling constant for the interaction between h and standard model particles.

Figure 3: Feynman rules (left) and Feynman diagram (right), showing the dark matter (χ) pair annihilation to standard model particles.

Using Feynman rules, the Figure 3 (right) shows the Feynman diagram for interactions between dark matter and standard model particles mediated by the standard model Higgs Boson. Reading the diagram from left to right in the direction of time, it shows a dark matter pair annihilating to produce two standard model particles. This process reduces the number density of dark matter, and so is relevant for evaluating dark matter abundance.

The final state standard model particle can be a W or Z boson, the standard model Higgs Boson, or a fermion. To show the process of calculating and evaluating cross-section, we focus on fermion final states in this project. The Feynman diagram for a dark matter pair annihilating to a fermion (f) and anti-fermion ($\bar{f}$) pair is shown below.

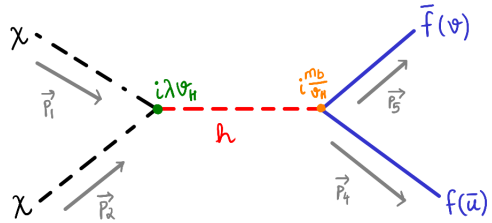

Figure 4: Feynman diagram for a pair of dark matter (χ) annihilating to standard model fermions $f, \bar{f}$ (mediated by the standard model Higgs Boson (h)).

In the above diagram, $\vec{p_1}, \vec{p_2}, \vec{p_3}, \vec{p_4}$ are the momenta in center of momentum frame associated with the initial and final states. The spinor wave functions associated with the outgoing fermion and anti-fermion $f, \bar{f}$ are given by $\bar{u}$ and v respectively. These form the solutions to the Dirac Equation. Since χ and h are scalars, the wave function associated with them is simply 1. The coupling constant λ governs interactions between χ and h, and $\frac{m_f}{v_h}$ governs interactions between h and $f, \bar{f}$, where $v_H = 246$ GeV, and m_f is the mass of the final state fermion.

We evaluate cross-section in the center of momentum frame. We can express the 4-momenta of the particles involved as

$$p_1 = \begin{pmatrix} E_1 \\ \vec{p_1} \end{pmatrix}, p_2 = \begin{pmatrix} E_2 \\ \vec{p_2} \end{pmatrix}$$
$$p_3 = \begin{pmatrix} E_3 \\ \vec{p_3} \end{pmatrix}, p_4 = \begin{pmatrix} E_4 \\ \vec{p_4} \end{pmatrix}$$

However, $\vec{p_1} = \vec{p_2} = 0$ since χ is at rest (dark matter is cold), and $\vec{p_3} = -\vec{p_4} = \vec{p_f}$, by conservation of momentum in the center of momentum frame. This gives

$$p_1 = \begin{pmatrix} E_1 \\ 0 \end{pmatrix}, p_2 = \begin{pmatrix} E_2 \\ 0 \end{pmatrix}$$
$$p_3 = \begin{pmatrix} E_3 \\ \vec{p_f} \end{pmatrix}, p_4 = \begin{pmatrix} E_4 \\ -\vec{p_f} \end{pmatrix}$$

By conservation of energy, we have $E_1 + E_2 = E_3 + E_4$. $E^2 = p^2 + m^2$, so $E_1^2 = E_2^2 = m_\chi^2$ and $E_3 = E_4$, because the fermion and anti fermion have the same mass. We conclude $E_3 = E_4$, and so $E_1 = E_2 = E_3 = E_4$.

To solve the Boltzmann equation, we need to evaluate $\langle \sigma v \rangle$, which is given by

$$\langle \sigma v \rangle = \frac{N_f p_f}{64\pi^2 \sqrt{s} E_1 E_2} \int \mathcal{M}_{sq} d\Omega$$

where, N_f is the number of color degrees of freedom of the outgoing particles, and $s = (p_1 + p_2)^2$, and $d\Omega$is the differential solid angle. $\mathcal{M}_{sq} \propto \mathcal{M}^\dagger \mathcal{M}$, where $\mathcal{M}$ is the scattering amplitude of the interaction and defines the probability of the process taking place. It can be read from the Feynman diagram in Figure 4and is expressed as

$$\mathcal{M} = \frac{2\lambda m_f}{(s - m_h^2) - i\Gamma_h m_h} [v\bar{u}]$$

where, v is the wave function associated with the outgoing anti-fermion, $\bar{u}$ is the wave function associated with the outgoing fermion, Γ_h is the total Higgs Boson decay width term, and m_h is the mass of the Higgs Boson.

$$\mathcal{M}_{sq} = \prod_\chi \frac{1}{2s_\chi + 1} \sum_{\text{spin}_f} |\mathcal{M}|^2$$

To evaluate $\mathcal{M}_{sq}$, we need to average over the spin of the incoming particles (since χ is a scalar, $s_i = 0$), and sum over the spin of the final state particles (fermions have spin $\frac{1}{2}$).

$$\mathcal{M}_{sq} = \sum_{\text{spin}_f} |\mathcal{M}|^2$$

We used the Feyncalc [11] package of Wolfram Mathematica [5] to obtain $\mathcal{M}_{sq}$.

$$\mathcal{M}_{sq} = \frac{16\lambda^2 m_f^2}{(s - m_h^2)^2 - \Gamma_h^2 m_h^2} (p_3 \cdot p_4 - m_b^2)$$

Now that we have $\mathcal{M}_{sq}$, we can evaluate $\langle \sigma v \rangle$.

For $s = (p_1 + p_2)^2 = 4m_\chi^2$ and our choice of dark matter mass, $m_\chi \ll \frac{1}{2}m_h^2$, the term in the denominator is approximately given by $s^2 - \Gamma_h^2 m_h^2 \approx s^2$, since the Higgs decay width is only a few MeV, whereas m_χ and m_h are both of order 100 GeV. Similarly, $p_3 \cdot p_4 = \frac{1}{2}(s - 4m_b^2) \approx \frac{s}{2}$, since $m_\chi \ll m_h$ (where $m_b \approx 4$MeV). This, along with the kinematic relations $s = (p_1 + p_2)^2 = 4m_\chi^2$ and $E_1 = E_2 = E_3 = E_4 = \frac{\sqrt{s}}{2}$ gives us a final result for the cross-section.

$$\langle \sigma v \rangle \approx \frac{\lambda^2 m_f^2}{\pi s^2} = \frac{\lambda^2 m_f^2}{16\pi m_\chi^4}$$

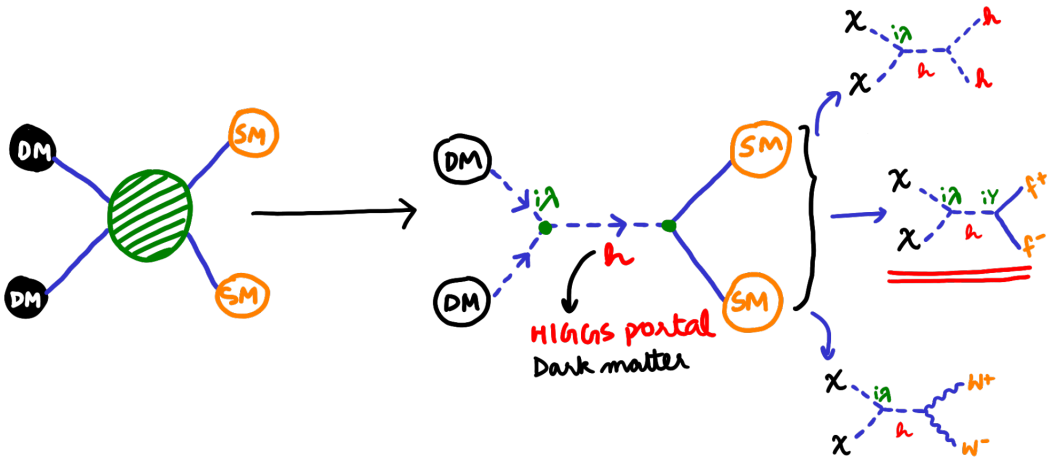

Figure 5: Annihilation of Higgs Portal dark matter to different standard model particles.

Two dark matter particles can decay into other standard model particles. Figure 5 shows some different possibilities for the annihilation of dark matter under a Higgs Portal model. A standard model channel opens up when a particle satisfies the kinematic threshold $m_\chi > m_h$ (since χ cannot annihilate into a particle that has greater mass than itself). The total cross-section is a function of dark matter and standard model particle mass and, and is a sum over all processes. It can be written as [4]

$$\langle \sigma v \rangle_{SM} = \sum_f \langle \sigma v \rangle \ \theta \ (m_\chi - m_{SM}),$$

where θ is a step function representing kinematic constraints, namely $\theta = 0$ for $m_\chi < m_{SM}$, and $\theta = 1$ for $m_\chi > m_{SM}$. For $m_\chi > 100$ GeV, we need to include the W, Z, and Higgs bosons in the sum, since they dominate the cross-section over fermions like the bottom and top quark. The cross-section formulae for these different processes are of the same order in the limit $s > 100$ GeV [4]. The total cross-section is approximately given by

$$\langle \sigma v \rangle = \frac{\lambda^2}{4\pi m_\chi^2}$$

When $m_\chi >> 100$ GeV, this cross-section is significantly greater than the cross-section for the case involving a bottom quark. Even for $m_\chi > m_{top} = 172.76$ GeV, the total cross-section is dominated by W, Z, and H boson modes. So, in our analysis, we consider the W, Z, and H cross-section for the total cross-section.

Now, our model has only two free parameters. The first is λ, or the coupling constant defining the strength of χ interactions with the Higgs Boson. The second is m_χ, or the mass of dark matter. With these as our input parameters, we are now prepared to solve the Boltzmann equation.

4 Solving the Boltzmann Equation

For this project, we obtained a solution for Higgs Portal dark matter by solving the Boltzmann equation with the relevant parameters, λ and m_χ. For the initial conditions, we consider a scenario where dark matter was in thermal equilibrium with other particles. This implies the condition $Y_x >> 1 = Y_{eq}$ for the Boltzmann equation. We solve the Boltzmann equation numerically using Wolfram Mathematica [5] and show our result in Figure 6.

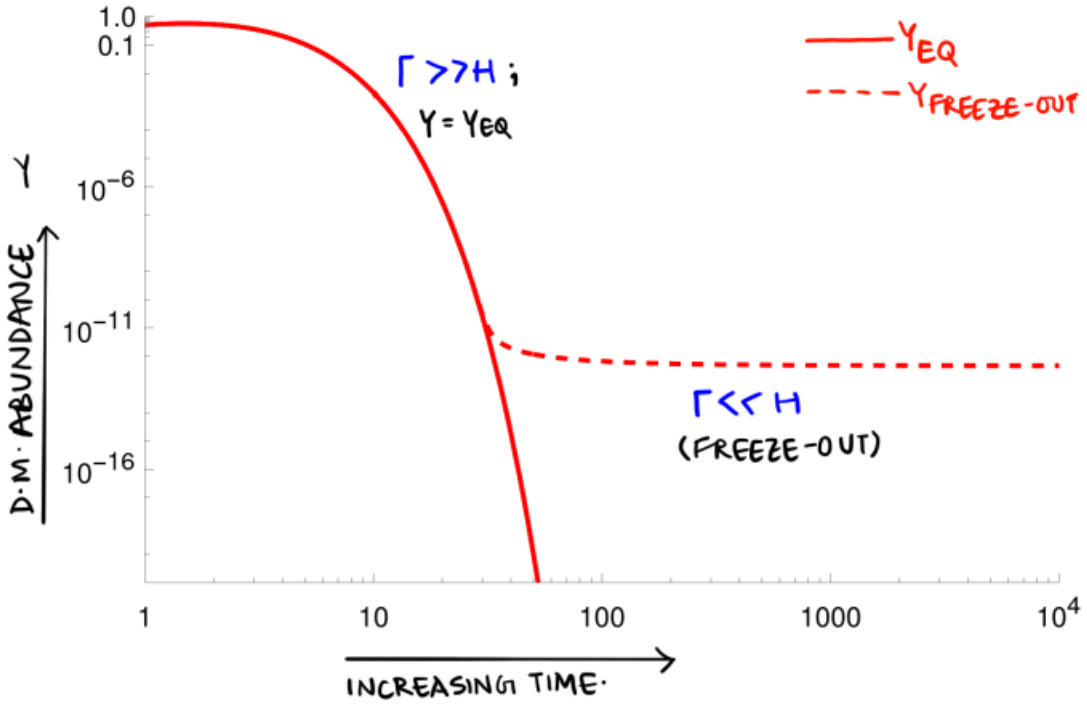

Figure 6: Solution to the Boltzmann equation under a freeze-out model for fixed m_χ and Γ.

Figure 6 shows the abundance of dark matter, Y, along the vertical and $x \propto t$ along the horizontal. When the interactions between particles is much stronger than the expansion of the universe, i.e. $\Gamma >> H$, this interaction is strong enough to maintain thermal equilibrium, which means the number of dark matter and standard model particles is equal (shown by overlapping lines for T_∞ in the figure, where the solid line shows abundance of standard model particles, and the dashed line shows abundance of dark matter particles). Mathematically, this implies $Y = Y_{eq}$.

At late times, $\Gamma < H(x)$, the expansion of the universe is greater than the interaction rate. Dark matter interactions become less frequent, and its abundance ($Y_{freeze-out}$, represented by the dashed line) decouples from the abundance of particles in thermal equilibrium and stays more or less constant. Beyond this point, the expansion of the universe prevents dark matter annihilation, resulting in the 'freeze-out' of dark matter abundance [7].

We can see the effect of Γ on the freeze-out, in Figure 7, we show Y as a function of x for increasing Γ. Since $\Gamma \propto \frac{\lambda^2}{m_\chi^2}$, greater Γ leads to stronger interaction between particles, which mean that dark matter is annihilating at a greater rate, leading to a smaller final abundance.

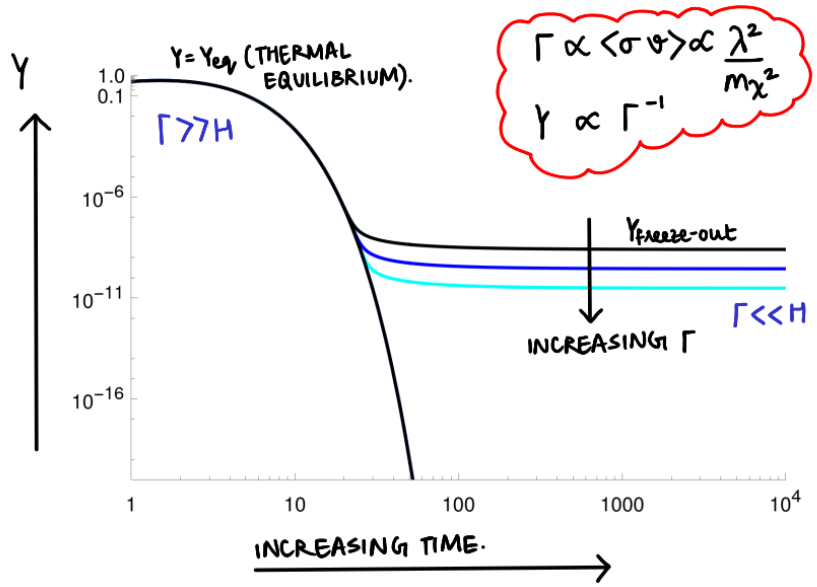

Figure 7: Solution to the Boltzmann equation under a freeze-out model and variation of solution with Γ

To illustrate the interplay between the coupling and dark matter abundance, we fix the mass of dark matter particles at, say, 1000GeV and then solve the Boltzmann equation for different coupling values. The horizontal lines in Figure 8 correspond to different abundance levels of dark matter in the universe. The graph shows that higher coupling values cause more dark matter annihilation, and lead to a smaller final abundance for a fixed m_χ. In terms of freeze-out dynamics, the dark matter with stronger coupling remains in thermal equilibrium for a longer time, which means the dark matter freezes out with a smaller abundance. See Figure 7 for an illustration of this idea.

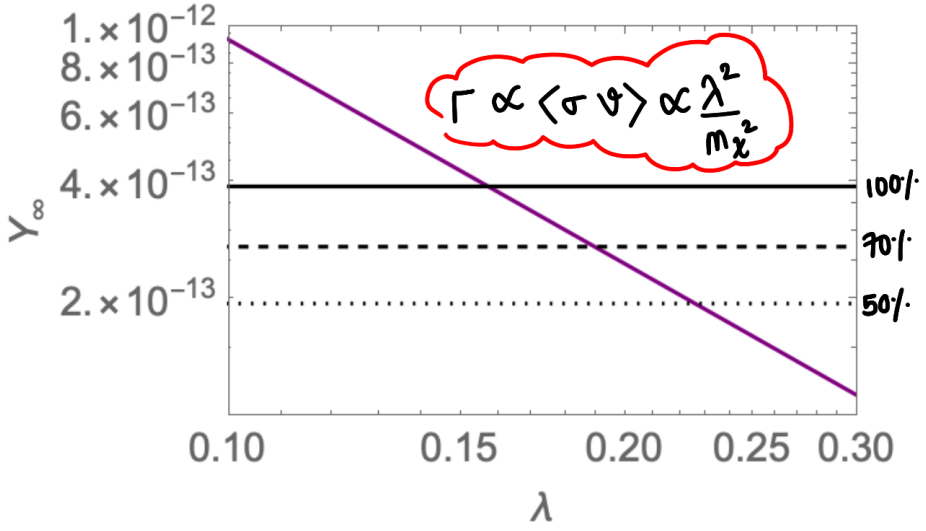

Figure 8: Solution to the Boltzmann equation under a freeze-out model for different abundance levels

Repeating this process for a range of values of m_χ, we get a set of λ values that correspond to each of our m_χ values. This tells us the relationship between m_χ and λ that is required to reproduce the desired abundance of dark matter in our universe.

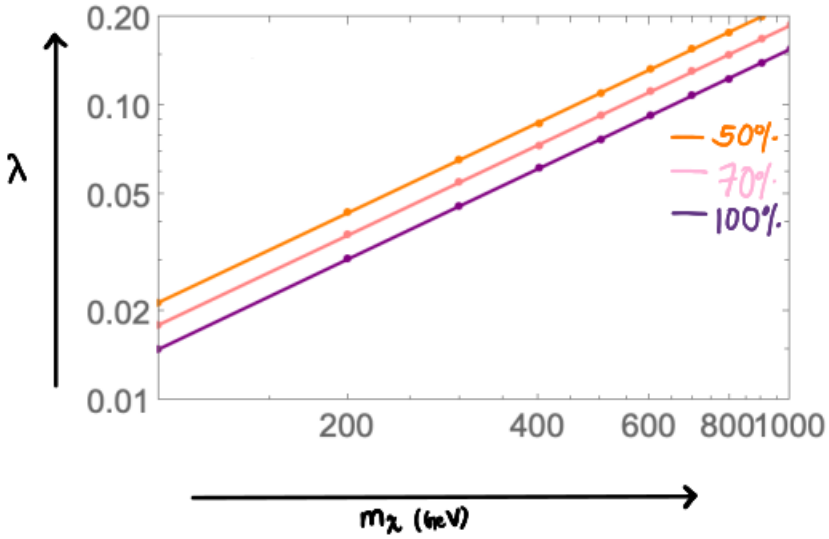

Figure 9: Plotting the relation between m and λ at different abundance levels.

This final result has been plotted in Figure 9, which shows the relation between λ and m_χ for different abundance levels of dark matter. For a fixed abundance, a higher m_χ requires larger coupling to reproduce the desired abundance of dark matter. Similarly, for fixed m_χ, a smaller abundance requires greater coupling. A higher coupling constant leads to stronger interactions between dark matter and standard model particles. This leads to more annihilation of dark matter, and so results in a smaller abundance of dark matter. Similarly, a higher m_χ leads to a smaller cross-section, and so leads to the abundance freezing out at a higher level.

5 Experimental Bounds on Cross-Section

Although billions of WIMPs (Weakly Interacting Massive Particles) through the Earth at any given second, they are extremely hard to detect due to their cold and dark nature, which leads to weak interactions. Efforts to detect WIMP dark matter using direct detection experiments aim to observe inelastic scattering between dark matter particles and heavy nuclei. This interaction causes a scintillation, or the emission of a light signal. The LZ direct detection experiment uses xenon nuclei. Results from LZ have set stringent bounds on the interaction cross-section, constraining the strength of the interaction between dark matter and standard model particles, namely, the nucleon of the Xenon atom [4][6].

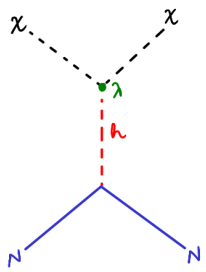

Figure 10: Feynman diagram for the interaction between WIMP dark matter (χ) and a heavy nucleon (N) Here, N is a proton or neutron-like particle made of quarks and gluons.

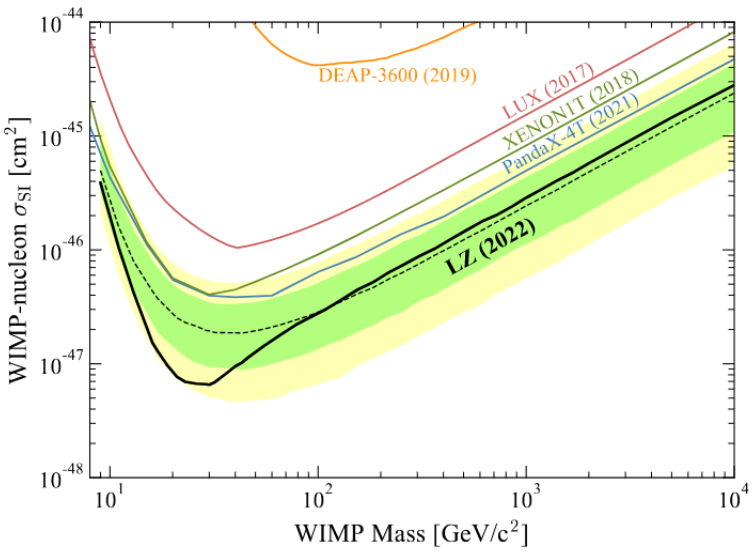

Figure 11: Plot showing bounds on cross-section set by direct-detection experiments. The region above the solid black line is excluded.[6]

In our case, χ is a spinless particle and the bound on the interaction is from the spin-independent interactions between the dark matter and heavy nucleons. The cross-section for this interaction is given by :

$$\sigma_{SI} \approx \frac{\lambda^2}{\pi m_h^4} \mu_{eff}^2 f_N^2$$

Here, λ is the coupling constant for the interaction between χ and h and m_h is the mass of the Higgs Boson [4]. The effective mass (μ_{eff}) of the system is given by $\frac{m_N m_\chi}{m_N + m_\chi}$, and $f_N^2 \approx 0.706 m_N^2$. The mass of the nucleus, m_N, is approximately equal to 0.939GeV.

The spin-independent cross-section for the interaction between dark matter and heavy nuclei depends on m_χ and λ. We can calculate the value of σ_{SI} for the ordered pairs of (m_χ, λ) we found in our previous result and compare it to the σ_{SI} bound found by the LZ experiment.

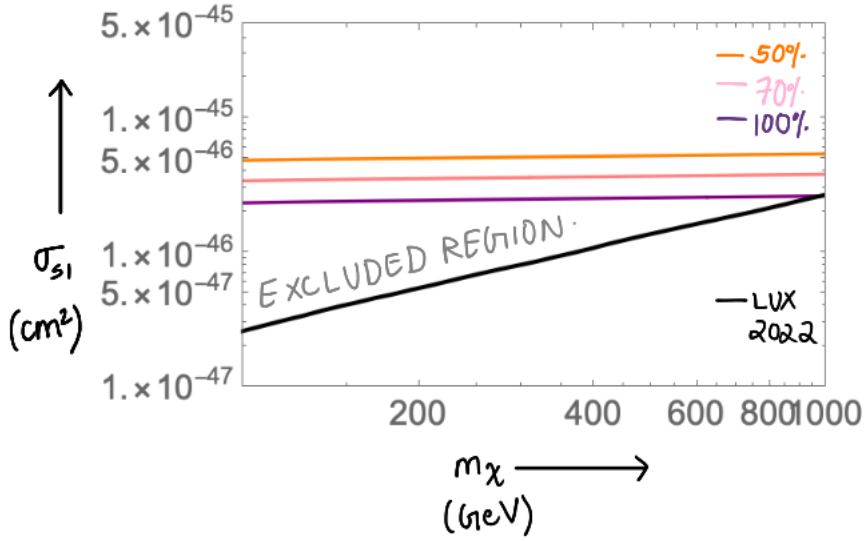

Figure 12: Plot comparing theoretical cross-section to the bound obtained by the LZ experiment[6].

In Figure 12, we see σ_{SI} as a function of mass for different values of dark matter abundance. The black line is the experimental bound, and the colored lines show the relation between σ_{SI} and m_χ from our result for different dark matter abundances shown in Figure 9.

All three of our theoretical cross-section curves almost lie above the experimental constraint, except for values of $m_\chi \approx 1000$ GeV for the 100% abundance case. This means the direct detection experiment has ruled out almost all the parameter space for $m_\chi > 100$ GeV. The situation is worse for smaller abundances, since for a given m_χ, a small final abundance requires a large coupling or spin-independent cross-section.

6 Discussion

In this section, we will focus on the case where $m_\chi < 100$ GeV to identify the parameter space that avoids the severe constraint from direct detection.

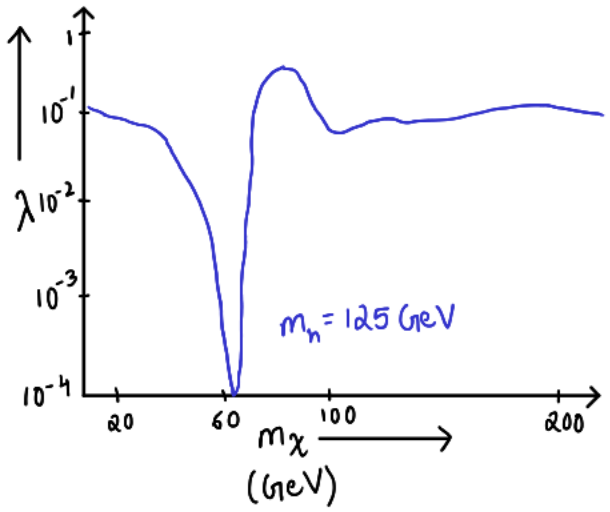

Figure 13: Plot showing relation between λ and m_χ for $m_\chi < 200$.[4]

To facilitate our discussion, in Figure 13 we have reproduced the result from Ref. [4]. Figure 13 shows λ as a function of m_χ needed to reproduce the observed dark matter abundance. The result for $m_\chi > 100$ GeV agrees with our result in Figure 10. For $m_\chi > 100$ GeV, we see a sharp drop in the coupling value when $m_\chi \simeq \frac{m_h}{2}$. To understand this behavior let us consider the dark matter annihilation cross-section when $s = 4m_\chi^2 = m_h^2$, or equivalently, $m_\chi \simeq \frac{m_h}{2}$,

$$\langle \sigma v \rangle \propto \mathcal{M}_{sq} = \frac{\lambda^2}{(s - m_h^2)^2 - \Gamma_h^2 m_h^2} = \frac{\lambda^2}{\Gamma_h^2 m_h^2}$$

Comparing this to our previous case, $s > m_h^2$, where

$$\langle \sigma \rangle \propto \frac{\lambda^2}{s^2} = \frac{\lambda^2}{m_\chi^4},$$

we see that the dark matter cross-section is significantly enhanced because $\Gamma_h m_h \ll m_\chi^2$. This phenomenon of enhancement of the cross-section is called resonance. A large cross-section leads to a smaller abundance of dark matter. We can overcome this suppression by choosing a λ value.

On the other hand, a small coupling value needed to reproduce the observed dark matter abundance leads to a significantly smaller spin-independent cross-section near resonance. In fact, one finds that the spin-independent cross-section near the resonance is small enough to evade the direct detection constraint [4]. In

Figure 14 we illustrate this effect by reproducing the result from [4] which shows the spin-independent cross-section as a function of m_χ. We have updated their result with the latest bound from the LUX experiment. The parameter region above the red curve is excluded. The plot shows that indeed the that the parameter region near resonance, $m_\chi = \frac{m_h}{2}$, is still allowed after imposing the direct detection constraints. Naively extrapolating the experimental and the theoretical lines, we can see that the two lines intersect at around $m_\chi \simeq 1000$ GeV. This agrees with our results in Figure 12.

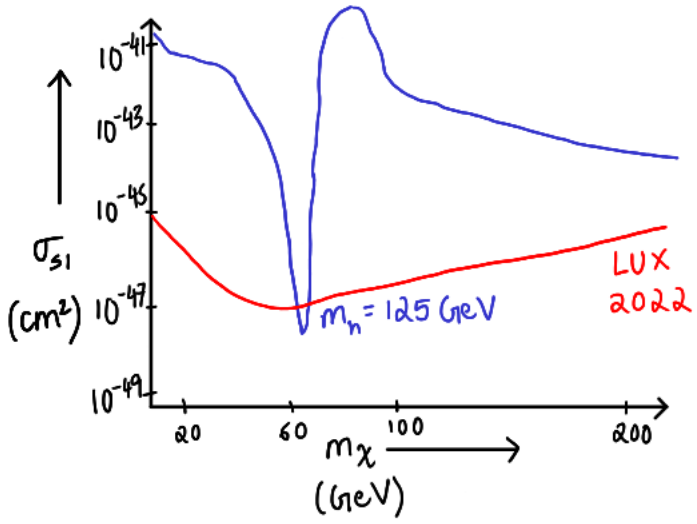

Figure 14: Plot showing relation between spin-independent cross-section and m_χ alongside experimental bound from direct-detection experiments.[4][6]

7 Conclusion

Although astrophysical and cosmological experiments estimate that dark matter constitutes about 85% of all matter in the universe, there is no viable dark matter candidate within the standard model of particle physics. One of the most popular dark matter candidates is so-called Higgs Portal dark matter. In this model, the standard model is extended to include a scalar particle that serves as a dark matter candidate. An additional symmetry is imposed, which forbids dark matter from interacting with any other standard model particle except for the Higgs Boson. All the interactions between dark matter and standard model particles are mediated by the standard model Higgs Boson, hence the name 'Higgs Portal' dark matter. Furthermore, this means that all dark matter interactions are determined by just 2 free parameters - the coupling constant (λ) for the interaction between dark matter (χ) and the standard model Higgs Boson, and the mass of dark matter (m_χ).

To evaluate the abundance of dark matter in the universe, we need to solve the so-called Boltzmann equation, which takes the cross-section of dark matter interactions with standard model particles as an input parameter. In the case of Higgs Portal dark matter, the cross-section quantifies the probability of dark matter annihilating to standard model particles. A larger cross-section leads to greater annihilation of dark matter and results in a smaller final abundance. Similarly, a smaller cross-section leads to less annihilation of dark matter and results in a larger final abundance.

For Higgs Portal dark matter, we have the total cross-section $\langle \sigma v \rangle \propto \frac{\lambda^2}{m_\chi^2}$, which includes standard model fermions, gauge bosons, and the Higgs Boson. As an example, we explicitly evaluated the cross-section formula for dark matter annihilating into standard model fermions. For a fixed m_χ, a large λ leads to a smaller abundance of dark matter at later times. To reproduce the current abundance of dark matter, λ is

uniquely determined for a fixed m_χ. This makes Higgs Portal dark matter a highly predictive and appealing model. We numerically solve the Boltzmann equation using Wolfram Mathematica to obtain λ as a function of m_χ for various abundance levels and $m_\chi > 100$ GeV.

Direct detection experiments look for signals from inelastic scattering between dark matter particles and heavy atomic nuclei like Xenon. These experiments place severe constraints on the cross-section for such interactions. For Higgs Portal dark matter, this cross-section is also determined by λ and m_χ. Using the λ and m_χ values obtained by solving the Boltzmann equation, we show that almost the entire parameter space for $100 < m_\chi \leq 1000$ GeV is ruled out by the experimental constraint.

Finally, we discuss the case of resonance, $m_\chi \approx \frac{m_h}{2}$, particularly focusing on how the parameter region around the resonance evades the direct detection bound. We discuss how the dark matter annihilation cross-section to the standard model particles is dramatically enhanced for $m_\chi \approx \frac{m_h}{2}$. Hence, in order to obtain the observed dark matter abundance for a fixed m_χ, a much smaller λ is required. A smaller λ leads to a much smaller inelastic scattering cross-section for the direct detection experiment. This reduced cross-section is small enough to avoid the direct detection constraint.

Acknowledgement

This project was funded by the John S. Toll Science and Mathematics Fellows program and the Cater Society of Junior Fellows. Special thanks to the instructors of Washington College's Department of Physics. None of this would have been possible without Dr. Thuecks' support and resourcefulness, Dr. Kehm's encouragement, and Dr. Shrestha's guidance and patience. I am particularly grateful to Dr. Stacy, Dr. Poulsen, Dr. Wilson, and Professor Andrews at the Department of Mathematics and Computer Science at Washington College for their advice and encouragement. I would also like to thank my friends at Washington College, whose encouragement and company kept me sane while I worked on this project. Thank you, Rano, Akshara, Tapas, Jason, Max, Eniya, Paleena, Adrienne, Faithlin, and Emily. I am grateful to Dr. Raut, my advisor, without whom this project would not have been possible. Thank you for being a wonderful and dependable mentor, teacher, and role model during this process. Finally, to Amma and Madhav, thank you for always being there.

References

[1] G. Bertone, D. Hooper, and J. Silk. Particle dark matter: evidence, candidates and constraints. *Physics Reports*, 405(5-6):279–390, Jan 2005.

[2] R. S. Ellis. Gravitational lensing: a unique probe of dark matter and dark energy. *Philosophical Transactions of the Royal Society A: Mathematical, Physical and Engineering Sciences*, 368(1914):967–987, 2010.

[3] D. Griffiths. *Elementary particle dynamics*. 1987.

[4] W.-L. Guo and Y.-L. Wu. The real singlet scalar dark matter model. *Journal of High Energy Physics*, 2010(10), oct 2010.

[5] W. R. Inc. Mathematica, Version 13.2. Champaign, IL, 2022.

[6] e. a. J. Aalbers. First dark matter search results from the LUX-ZEPLIN (LZ) Experiment. 2022.

[7] E. W. Kolb and M. S. Turner. *The Early Universe*, volume 69. 1990.

[8] M. Lisanti. Lectures on dark matter physics. In *New Frontiers in Fields and Strings*. WORLD SCIENTIFIC, nov 2016.

[9] e. a. N. Aghanim. Planck 2018 results. *Astronomy & Astrophysics*, 641:A6, sep 2020.

[10] V. C. Rubin, J. Ford, W. K., and N. Thonnard. Rotational properties of 21 SC galaxies with a large range of luminosities and radii, from NGC 4605 (R=4kpc) to UGC 2885 (R=122kpc). , 238:471–487, June 1980.

[11] V. Shtabovenko, R. Mertig, and F. Orellana. FeynCalc 9.3: New features and improvements. *Computer Physics Communications*, 256:107478, nov 2020.

[12] F. Tanedo. Defense against the dark arts. *Notes on dark matter and particle physics*, 2011.